

## **SPATIAL CORRELATION OF GROUND MOTIONS IN THE 2016-2017 CENTRAL ITALY SEISMIC SEQUENCE**

Erika SCHIAPPAPIETRA<sup>1</sup>, John DOUGLAS<sup>2</sup>

**Abstract:** Over the past decade, spatial correlation of earthquake ground motion has become increasingly important for seismic hazard and risk assessments, particularly when applied to portfolios of buildings or spatially distributed infrastructures. Indeed, not only do these studies require the estimation of ground motion intensity measures at multiple sites, but also the quantification of the correlation structure.

Several spatial correlation models have been published and common findings suggest that intra-event correlation decreases quite rapidly with increasing separation distances. Nevertheless, significant differences among the proposed models exist, leading to large uncertainties in the assessed seismic risk. This suggests that different correlation estimation methods, earthquake type and magnitude, as well as region and local site conditions might play first-order roles in the observed differences.

The aim of this study is to identify factors that influence the correlation structure of ground-motion measures and quantify the variability of spatial correlation among different events within the same region and with the same local site conditions. In order to investigate this, we carry out a thorough geostatistical analysis of the intra-event correlation structure, taking advantage of the 2016-2017 Central Italy seismic sequence database, which include nearly 1,600 records from nine  $M_w \geq 5.0$  events that occurred over a time period of five months.

Our preliminary results could be used to improve seismic loss estimation as well as for more informed risk management and decision making in this region.

### **Introduction**

The seismic risk assessment of spatially distributed urban infrastructures and buildings is of paramount importance for more informed risk management and decision making designed to reduce economic and human losses (Weatherill *et al.*, 2014, 2015). Conversely to seismic risk analysis of a single structure, these studies require not only the estimation of ground motion intensity measures (IMs) at multiple sites during the same earthquake, but also the quantification of the correlation structure (Goda and Atkinson, 2009, 2010; Jayaram and Baker, 2009; Esposito and Iervolino, 2011, 2012; Weatherill *et al.*, 2014, 2015; Wagener *et al.*, 2016; Heresi and Miranda, 2018). Traditional seismic hazard and risk analysis techniques often determine the ground motion caused by an earthquake through ground motion prediction equations (GMPEs). GMPEs provide an estimate of the ground shaking and its associated aleatory variability at a given site, without any insight on the spatial correlation of the IM of interest. Besides, conventional tools are grounded on the hypothesis of considering independent IMs at different sites. However, modelling the joint IMs prediction, and thus defining the spatially correlated random ground motion fields, is a fundamental prerequisite for the assessment of earthquake effects on a region (Goda and Atkinson, 2009; Jayaram and Baker, 2009; Esposito and Iervolino, 2011). Park *et al.* (2007) and Sokolov and Wenzel (2011) demonstrated that neglecting the spatial correlation may cause bias in loss estimation, overestimating the most likely losses and leading to differences in the prediction of up to 40%.

The generation of a spatially correlated ground motion field is a demanding task (Weatherill *et al.*, 2014), and over the past decade studies on spatial correlation have played an increasingly important role. Several models have been published and common findings suggest that: (1) intra-event correlation decreases quite rapidly with increasing separation distances, and (2) ground motion IMs associated to lower frequencies feature larger correlation (Goda and Hong, 2008;

---

<sup>1</sup> Ph.D. Student, Department of Civil and Environmental Engineering, University of Strathclyde, Glasgow (UK), erika.schiappapietra@strath.ac.uk

<sup>2</sup> Chancellor's Fellow (Lecturer), Department of Civil and Environmental Engineering, University of Strathclyde, Glasgow (UK)

Jayaram and Baker, 2009; Esposito and Iervolino, 2012; Wagener *et al.*, 2016). Nevertheless, significant differences among the proposed models exist, leading to large uncertainties in the assessed seismic risk. This suggests that different correlation estimation methods, earthquake type and magnitude, as well as region and local site conditions play first-order roles in the observed differences.

The aim of this study is to identify factors that influence the correlation structure of ground-motion measures and quantify the variability of spatial correlation among different events when the same seismic region is considered. In order to investigate these factors, we carry out a geostatistical analysis of the intra-event correlation structure using the 2016-2017 Central Italy seismic sequence database, which includes nearly 1,600 records from nine  $M_w \geq 5.0$  events that occurred over a time period of five months.

### Intra-event spatial correlation model

The correlation of ground motion IMs from an earthquake includes three main elements, namely: (1) the spatial correlation between intra-event residuals of the same IM for adjacent sites; (2) the correlation between intra-event residuals of different IM at the same location; and (3) the spatial cross-correlation between intra-event residuals of different IM for closely spaced sites (Weatherill *et al.*, 2015). This study focuses on the first of the above-mentioned elements.

In general, the similarity of ground motion IMs at two different sites depends on: (1) the earthquake; (2) the propagation path from the source to the sites; (3) the position of closely spaced sites in near-source conditions with respect to the main fault asperities (Park *et al.*, 2007). The first of these aspects is commonly accounted for by the inter-event residual term provided by the GMPE. GMPEs relate a ground motion IM (e.g. peak ground acceleration, PGA; peak ground velocity, PGV; peak ground displacement, PGD; or pseudo-spectral acceleration for 5% of critical damping, SA) to a set of explanatory variables describing the source (e.g. magnitude and focal mechanism), wave propagation path (e.g. distance metric and regional effects) and site response (e.g. soil classification) (e.g. Douglas and Edwards, 2016). In general, such parameters are modelled as lognormally distributed random variables; therefore, GMPEs take the form:

$$\text{Log}_{10} Y_{ij} = \text{Log}_{10} \bar{Y}_{ij}(M, R, S, \delta) + \varepsilon_{ij} + \eta_j \quad (1)$$

where  $Y_{ij}$  is the IM of interest at the  $i^{\text{th}}$  site due to the  $k^{\text{th}}$  event, whereas  $\bar{Y}_{ij}$  is the predicted median function of magnitude ( $M$ ), distance from the source ( $R$ ), local-site conditions ( $S$ ) and others explanatory variables ( $\delta$ ).  $\varepsilon_{ij}$  and  $\eta_j$  are the intra-event and inter-event residual terms, respectively. It is assumed that these terms are independent and normally distributed random variables with zero mean and standard deviation  $\sigma_\varepsilon$  and  $\sigma_\eta$ , respectively. The inter-event component denotes the variability between different earthquakes and does not depend on the site. Conversely, the intra-event component is site dependent as it accounts for differences from the average model due to the path and local site effects. Consequently, the total residual terms  $\varepsilon_{ij} + \eta_j$  provide insight only on the intra-event spatial correlation, being  $\eta_j$  constant across all sites when a single event is considered (Jayaram and Baker, 2009; Heresi and Miranda, 2018).

Generally, either an existing GMPE or an *ad hoc* regression model are used to compute the intra-event residuals at each site in order to assess the intra-event spatial correlation  $\rho_\varepsilon(h)$ . This can be estimated with two different approaches, namely: (1) computing directly the covariance and the correlation coefficient (e.g. Wang and Takada, 2005; Sokolov *et al.*, 2010); or (2) calculating the sample semivariogram (e.g. Jayaram and Baker, 2009; Goda and Atkinson, 2010; Esposito and Iervolino, 2011, 2012; Heresi and Miranda, 2018). It is worth mentioning that we assume the hypothesis of stationarity and isotropy, so that the expected value of the random variable is constant for all the sites and the covariance depends only on the separation distance between two sites and not on their absolute position.

In the first method, the spatial correlation is estimated as:

$$\rho_\varepsilon(h) = \frac{\text{COV}[\varepsilon_{ij}, \varepsilon_{kj}]}{[\sigma_\varepsilon]^2} \quad (2)$$

where COV denotes the covariance function, whereas  $\varepsilon_{ij}$  and  $\varepsilon_{kj}$  are the intra-event variability for the site  $i^{\text{th}}$  and  $k^{\text{th}}$  during the  $j^{\text{th}}$  event with zero mean and standard deviation  $\sigma_\varepsilon$ .

The second method implements two different estimators:

1. Method of moments (Matheron, 1962)

$$\hat{\gamma}(h) = \frac{1}{2N(h)} \sum_{N(h)} \{ \varepsilon'_{ij} - \varepsilon'_{kj} \}^2 \quad (3)$$

where  $N(h)$  represents the number of pairs separated by  $h$ . Following Jayaram and Baker (2009),  $\varepsilon'_{ij}$  denotes the normalized intra-event residual with respect to the standard deviation of the intra-event residual at the  $i^{\text{th}}$  site.

2. Estimator proposed by Cressie and Hawkins (1980)

$$\hat{\gamma}(h) = \frac{1}{2} \left\{ \frac{\left[ \frac{1}{N(h)} \sum_{N(h)} |\varepsilon'_{ij} - \varepsilon'_{kj}|^{0.5} \right]^4}{0.457 + \frac{0.494}{N(h)}} \right\} \quad (4)$$

Both the covariance and the semivariogram are calculated for each pair of stations  $(x_i, x_j)$  whose inter-site spacing falls in a distance bin defined as  $h - \Delta h / 2 \leq |x_i - x_j| \leq h + \Delta h / 2$ . In this study we select a bin size of 4 km in order to have at least 30 pairs per bin as proposed by Esposito and Iervolino (2011, 2012). Furthermore, the definition of  $\sigma_\varepsilon$  is of primary importance; indeed, it can be estimated either from the sample semivariogram at large separation distances, where the intra-event residuals are assumed to be uncorrelated, or as the standard deviation of the intra-event residuals for a given event (Goda and Atkinson, 2010). Alternatively, Esposito and Iervolino (2011) employ the standard deviation related to the GMPE as  $\sigma_\varepsilon$ . However, this approach is strongly discouraged by Heresi and Miranda (2018) who assert that using a constant value of  $\sigma_\varepsilon$  for different events might lead to a biased intra-event correlation. The experimental values must be fitted to a theoretical functional form to retrieve semivariogram values for any distance  $h$ . We employ an exponential model that takes the form:

$$\gamma(h) = a[1 - \exp(-3h / b)] \quad (5)$$

so that the hypothesis of a stationary and isotropic field is fulfilled.  $a$  and  $b$  are the sill and the range of the semivariogram, respectively. The sill equals the variance of the data, whereas the range represents the distance over which the correlation between sites is negligible. The range is given as the distance at which  $\gamma(h)$  equals 0.95 times the sill. It is worth mentioning that the sill should be equal to 1 as the normalized intra-event residuals have a unit variance (Jayaram and Baker, 2009). It has been demonstrated (e.g. Webster and Oliver, 2007) that the semivariogram is related to the correlation coefficient, so that:

$$\gamma(h) = a[1 - \rho(h)] \quad (6)$$

Consequently, assuming  $a = 1$  due to the normalization, we have that:

$$\rho(h) = \exp(-3h / b) \quad (7)$$

In this study, we employ the approach based on the semivariogram to infer the range, after verifying that the covariance method provides similar results. The results are not reported here due to the limited space.

## Strong motion network and data

Starting from 24<sup>th</sup> August 2016, one of the most important seismic sequences ever recorded in Italy struck the Central Apennines between the municipalities of Amatrice and Norcia, causing widespread damages, thousands of homeless and invaluable losses for the historical heritage of the region. The first mainshock (Mw 6.0) struck on August 24<sup>th</sup> 2016 at 01:36 UTC near Amatrice and it was followed, within less than an hour, by a Mw 5.4 aftershock (Chiaraluce *et al.*, 2017). After two months, two other large earthquakes occurred: a Mw 5.9 on October 26<sup>th</sup> 2016 at 19:18 UTC, near the village of Ussita and a Mw 6.5 on October 30<sup>th</sup> 2016 at 06:40 UTC with epicentre close to Norcia (Luzi *et al.*, 2017). Four other Mw  $\geq 5.0$  earthquakes occurred on January 18<sup>th</sup> 2017 near the villages of Campotosto and Montereale (Figure 1). Origin times, hypocentral coordinates and magnitude for these events are listed in Table 1. The seismic sequence affected

an area characterized by NW-SE striking normal and normal oblique faults, consistent with the SW-NE extension measured by GPS stations in this sector of the Apennines (Cheloni *et al.*, 2016). In the past decades, the area has been struck by other large magnitude events, such as the 1984 Mw 5.6 Gubbio earthquake, the 1997 Mw 6.0 Colfiorito earthquake and the 2009 Mw 6.3 L'Aquila earthquake. All the events were recorded by about 250 stations mainly belonging to: the Italian strong-motion network (Rete Accelerometrica Nazionale, RAN), operated by the Italian Department of the Civil Protection (DPC), the Italian National Seismometric Network (INSN), operated by the Istituto Nazionale di Geofisica e Vulcanologia (INGV), and a temporary network of strong motion stations installed by INGV and DPC after the Mw 6.0 Amatrice earthquake (Luzi *et al.*, 2017). Temporary stations were set up to monitor the seismic sequence at a higher resolution and to retrieve more accurate observations of the ground shaking in the near-source region (Luzi *et al.*, 2017).

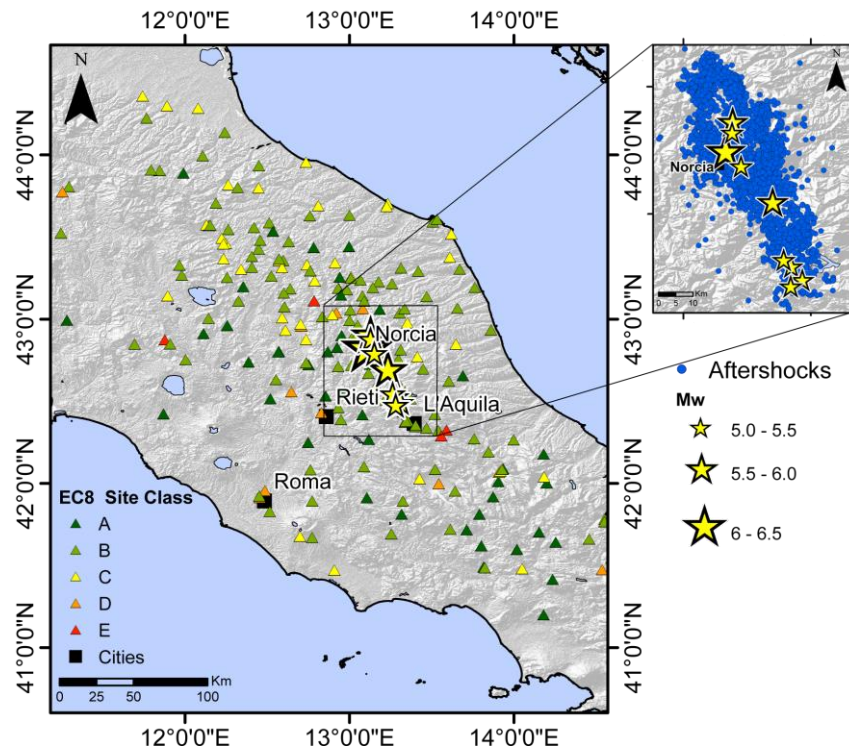


Figure 1. Epicentral locations (yellow stars) of the nine  $M_w \geq 5$  earthquakes of the sequence. Strong-motion stations (triangles) are also mapped and color-coded following the EC8 soil classification. In the zoom-view the epicentral locations are reported along with the  $M_w \geq 2.5$  aftershocks for one year after the Amatrice mainshock. Events and stations metadata are from Lanzano *et al.* (2018).

Event	Event Time	Latitude [°]	Longitude [°]	Depth [km]	Mw	# Records
Amatrice	24/08/2016 01:36	42.7	13.23	8.1	6.0	158
Amatrice Aftershock	24/08/2016 02:33	42.79	13.15	8	5.3	138
Visso I	26/10/2016 17:10	42.88	13.13	8.7	5.4	158
Visso II	26/10/2016 19:18	42.91	13.13	7.5	5.9	166
Norcia	30/10/2016 06:40	42.83	13.11	9.2	6.5	159
Monte Reale I	18/01/2017 09:25	42.55	13.26	9.2	5.1	127
Monte Reale II	18/01/2017 10:14	42.53	13.28	9.1	5.5	141
Pizzoli I	18/01/2017 10:25	42.49	13.31	8.9	5.4	129
Pizzoli II	18/01/2017 10:33	42.48	13.28	10	5.0	124

Table 1. Main characteristics of the largest magnitude events of the Central Italy sequence. [source: Lanzano *et al.* (2018)].

In this study we select data from 232 strong-motion stations within an epicentral distance of 200 km. Events and stations metadata are from Lanzano *et al.* (2018). The site conditions at each recording site are expressed through the EC8 subsoil categories (Eurocode 8, 2005), which is based either on the average shear-wave velocity of the upper-most 30 m ( $V_{s,30}$ ) or on the available geological information. For all those stations without an estimate of the  $V_{s,30}$ , we assume the  $V_{s,30}$  values inferred from the slope, using the approach of Wald and Allen (2007), as included in the ESM flat-file (Lanzano *et al.* 2018).

## Evaluation of the intra-event spatial correlation

### Computation of the semivariogram

We apply the procedure previously described to all the  $M_w \geq 5.0$  earthquakes of the 2016-2017 Central Italy seismic sequence. We use the geometric mean of the two horizontal components of PGA and 5%-damped SA at periods of vibration equal to 0.2, 0.5, 1, 2, 3 and 4s. For each event, we develop a ground motion model based on the observations in order to avoid any dependency on the chosen GMPE. We decided not to account for different local site conditions in this preliminary analysis; thus, the equation is:

$$\text{Log}_{10} Y_{ij} = b_1 - b_2 \text{Log}_{10} \sqrt{r_{rup,ij}^2 + b_3^2} \quad (8)$$

where  $Y_{ij}$  is the PGA or SA(T) expressed in  $\text{cm/s}^2$  and  $r_{rup}$  is the rupture distance (or the hypocentral distance for those events where the fault plane is not defined and the point-source approximation holds).  $b_1$ ,  $b_2$  and  $b_3$  are the model coefficients inferred through a 1-stage ordinary regression (which is justified as only data from a single earthquake are used). Figure 2a illustrates, as an example, the PGA model obtained for the Mw 6.5 Norcia earthquake and Figure 2b shows the spatial distribution of the intra-event residuals computed as  $\text{Log}_{10} Y_{ij} - \text{Log}_{10} \bar{Y}_{ij}$ .

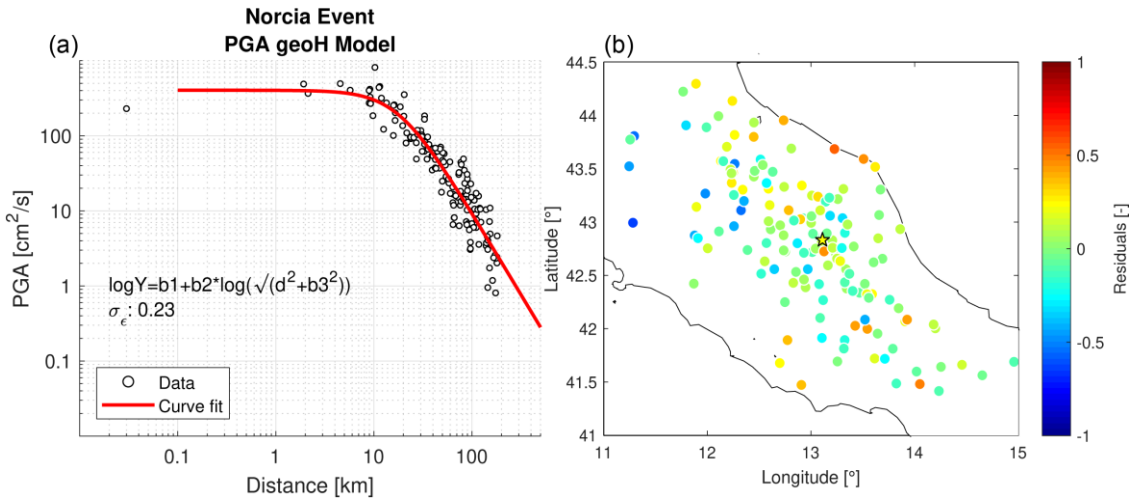


Figure 2. (a) GMPE fitted to the PGA values of the Norcia event; (b) Intra-event residuals obtained from the PGA data of the Norcia event.

We evaluate the sample semivariogram through equations (3) and (4) in order to compare the performance of both the estimators and we fit the values using equation (5). As already mentioned, the intra-event correlation is strongly affected by the intra-event standard deviation; therefore, its estimation is crucial (Goda and Atkinson, 2010; Sokolov *et al.*, 2012). In light of this, we consider two alternative values inferred from both the sample semivariogram at large separation distances and the intra-event standard deviation of regression residuals. The model parameters are retrieved through a weighted least squares method; the weights are computed depending on the inverse of the number of station pairs in each bin, so that smaller separation distances are weighted higher. Figure 3 summarises the outcomes for SA (1 s) for the Norcia event. The observed trends feature a decreasing degree of spatial dependence with increasing separation distance, as supported by the literature. Furthermore, in this case, the two  $\sigma_\epsilon$  values are almost identical; consequently, the inferred ranges are very similar. However, alternative estimates of the correlation distances based on  $\sigma_\epsilon$  computed from both regression residuals and semivariogram feature slightly different values (Figure 4). This discrepancy may partly be

explained by: (1) the subjectivity on the definition of large separation distance; (2) the correlation among residuals of closely spaced sites (Goda and Atkinson, 2010; Sokolov *et al.*, 2012).

Besides, we notice discrepancies on the outcomes obtained using equation (3) and (4) for the evaluation of the sample semivariogram. This might be because the estimator of Cressie and Hawkins is less sensitive to outliers (Esposito and Iervolino, 2011).

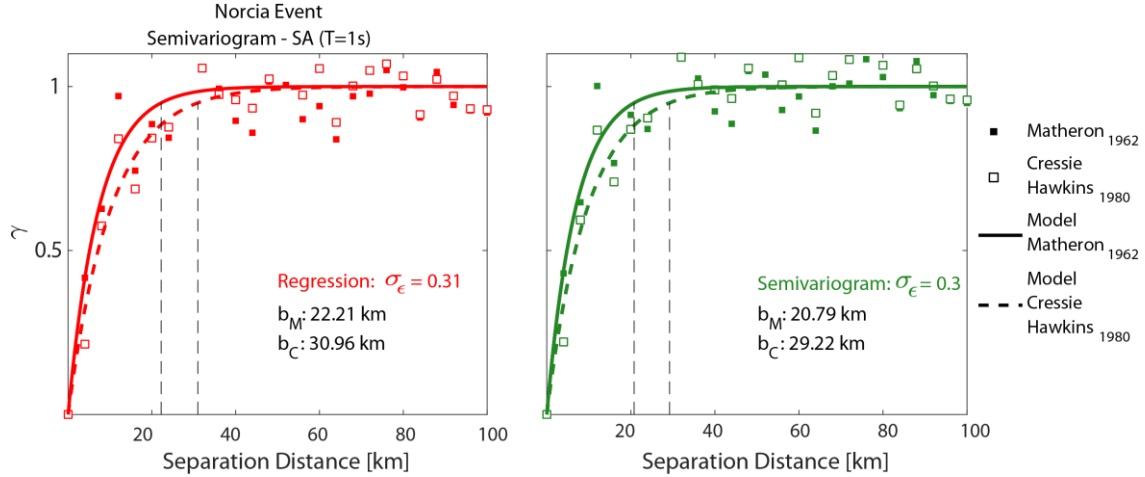


Figure 3. Semivariogram fitted to the data of the Norcia event for SA (1s), using both the estimator of Matheron (1962) and Cressie and Hawkins (1980): (a)  $\sigma_\epsilon$  is the standard deviation of the intra-event residuals for a given event; (b)  $\sigma_\epsilon$  is estimated as the sample semivariogram at a large separation distance.

#### Relationship between range and magnitude

The relation between the magnitude and the range is one of the most controversial points in ground motion correlation. Some authors (e.g. Sokolov *et al.*, 2012; Heresi and Miranda, 2018) argue that the correlation distance tends to increase with increasing magnitude because larger events are characterized by lower frequency contents. Conversely, other studies (e.g. Jayaram and Baker, 2009) did not find any correlation between these two parameters. Figure 4 compares the ranges obtained for each earthquake as a function of magnitude. The outcomes are rather surprising. The largest correlation distances are detected for the four events that occurred in January 2017, which have small magnitudes, whereas the largest earthquake shows quite a short range. On the contrary, the results obtained for the first four events (Amatrice mainshock and aftershock and Visso I and II) support the hypothesis of a positive correlation between the range and the magnitude.

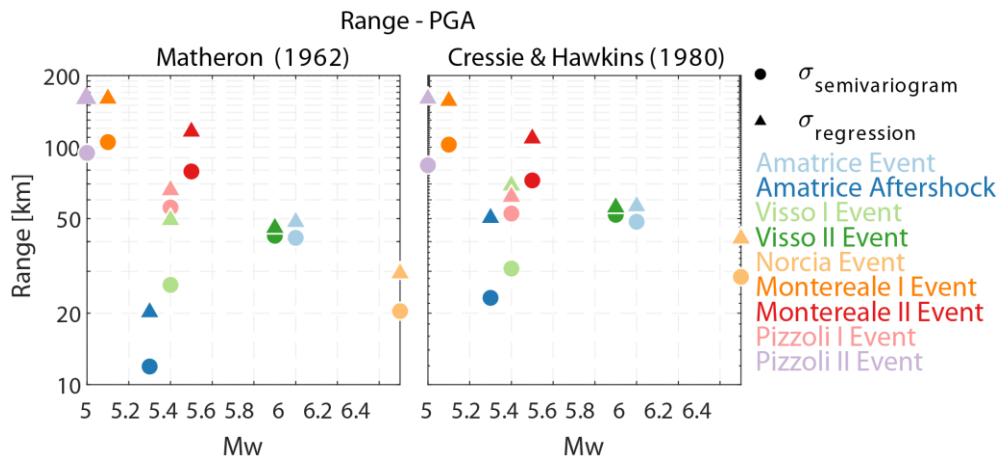


Figure 4. Range as a function of  $M_w$  for PGA.

To interpret our outcomes, we analyse both the spatial variations of the  $V_{s30}$  values and the spatial distribution of the residuals. The intra-event spatial correlation is understood as a non-random component in the residuals, which arises from neglecting a number of factors in the GMPEs, such



as soil conditions, path and azimuth as well as hanging-wall and foot-wall effects (Sokolov *et al.*, 2012). Jayaram and Baker (2009) studied the relation between the correlation of PGA residuals and  $V_{s30}$  values, arguing that a correlation between  $V_{s30}$  measurements, which reflects homogeneous site effects, leads to a larger correlation between PGA residuals. Indeed, if local site effects are not properly described by the GMPE, adjacent sites will be affected by analogous prediction errors that will influence the spatial correlation. We compute the semivariogram of  $V_{s30}$  values for each earthquake, following the same approach described for PGA residuals. The inferred correlation distances feature some differences, as the number and type of the considered stations vary for each event. Nevertheless, the results reveal a correlation between  $V_{s30}$  values, which can partially explain the differences in the PGA ranges. It is worth mentioning that most of the  $V_{s30}$  values are inferred from topographic slope and only about 30% of the values are measured; therefore, uncertainties in the  $V_{s30}$  estimation may have affected these outcomes. Moreover, deeper analysis on this aspect are required, as Heresi and Miranda (2018) demonstrated that the spatial correlation of  $V_{s30}$  does not provide evidence of the range variability.

Furthermore, we study the spatial distribution of both the recording stations with respect to the fault plane and the residuals. The low intra-event correlation found for the largest event of the sequence might be related to the characteristics of the ground motion in near source conditions, which feature a small-scale spatial variability due to the heterogeneous rupture process. Indeed, this is the only event that was recorded by stations within 5 km from the rupture plane. Besides, we analyse the mean and the standard deviation of the intra-event residuals to explain the very large ranges retrieved for the four earthquakes that occurred in January 2017. Interestingly, the intra-event residual shows a positive average value, in contrast to the Mw 6.0 Amatrice or Mw 6.5 Norcia events which have a zero mean. Figure 5 provides a comparison between the spatial distribution of the intra-event residuals of the Mw 6.0 Amatrice and Mw 5.5 Montereale II events. Figure 5b highlights a clear trend: two main clusters can be recognized where closely spaced stations have similar values. In particular, negative values are found to the south of the epicentre, whereas positive values occur to the north of the fault plane. Conversely, no clearly defined patterns are observed in Figure 5a and Figure 2b. A possible explanation for this outcome may be the presence of a high non-random component in the residuals, which reflects factors that are neglected in the GMPE. In particular, the frequency content of the ground motion, path or azimuthal effects along with site and geological conditions may play a first-order role in defining the intra-event spatial correlation. Moreover, the same earthquakes feature a higher  $\sigma_\epsilon$  with respect to the other events of the sequence. This may contribute to the large correlation distances. Sokolov *et al.* (2012) demonstrated that decreasing the non-random component in the residuals leads to a reduction of the correlation and the intra-event standard deviation. Therefore, further analyses are required to draw more firm conclusions on the range variability.

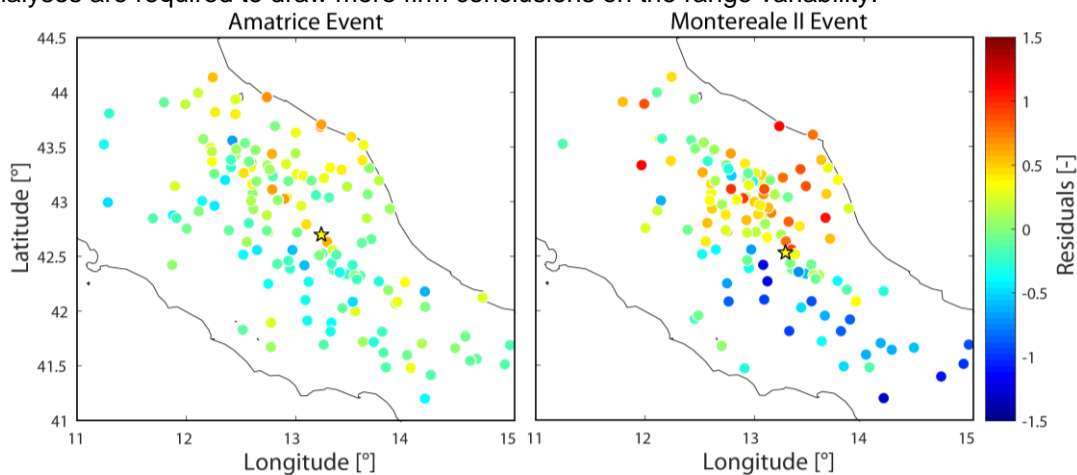


Figure 5. Spatial distribution of the intra-event residuals: (a) Mw 6.0 Amatrice event; (b) Mw 5.5 Montereale II event.

#### Relationship between range and period of vibration

It has been demonstrated (e.g. Esposito and Iervolino, 2012; Sokolov *et al.*, 2012; Wagener *et al.*, 2016) that spatial correlation distances are affected by the structural vibration period considered, and that range and frequency are inversely proportionate. Zerva and Zervas (2002) investigated the spatial coherency of ground motion and corroborated the hypothesis that the

small-scale heterogeneities in the travel path strongly influence the short-period waves (short wavelengths), in contrast to the low-frequencies waves. As it can be observed in Figure 6, our results agree with those from the literature. In some cases, the comparison between PGA and SA at periods up to 0.5 s show very similar ranges, as also shown by Wagener *et al.* (2016). Moreover, for most events the PGA ranges are larger than those obtained for SA at longer periods. This was found in the case of the Mw 7.6 1999 Chi Chi earthquake by Jayaram and Baker (2009), who explained this behavior by clustering of the  $V_{s30}$  values.

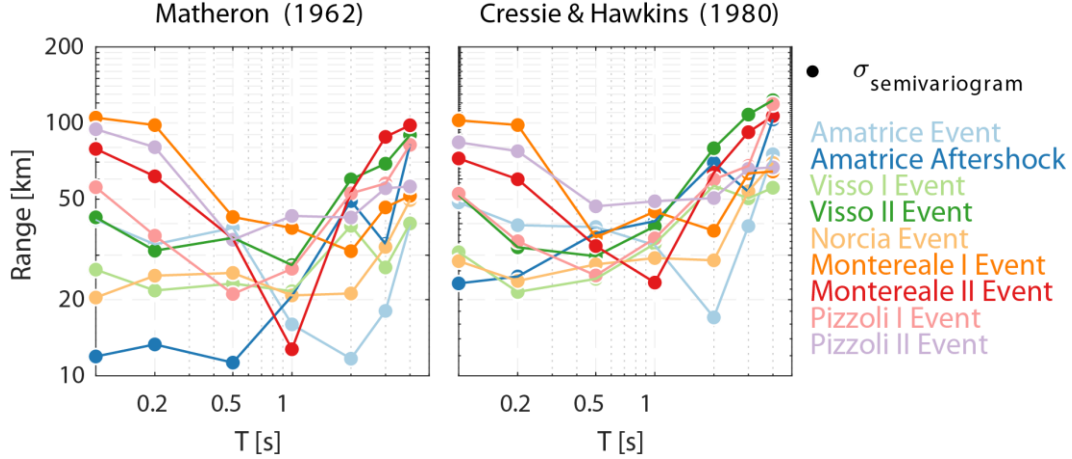


Figure 6. Range as a function of the structural period, using both the estimator of Matheron (1962) and Cressie and Hawkins (1980).  $\sigma_e$  is estimated as the sample semivariogram at large separation distances.

#### Comparison with other intra-event correlation models

Over the past decade, studies on spatial correlation have played an increasingly important role. Several models have been published and common findings suggest that: (1) intra-event correlation decreases quite rapidly with increasing separation distances, and (2) ground motion IMs associated to lower frequencies feature larger correlation (Goda and Hong, 2008; Jayaram and Baker, 2009; Esposito and Iervolino, 2012; Wagener *et al.*, 2016). Nevertheless, significant differences on the rate of correlation decay among the proposed models exist. The main reasons lie with: (1) datasets (single event, multiple events); (2) component of the ground motion and attenuation model (GMPE or *ad hoc* regression analysis); (3) approach used to compute the correlation distance (semivariogram or covariance); and (4) method of estimating  $\sigma_e$ . In Figure 7 we compare our correlation models for each analysed event with some of the models reported in literature. In particular, we select the models of Jayaram and Baker (2009); Goda and Atkinson (2010); Esposito and Iervolino (2012); and Heresi and Miranda (2018). All the analysed earthquakes (except for the four events that occurred in January 2017) show a rate of decay which falls between the two models proposed by Jayaram and Baker (2009), based on the  $V_{s30}$  clustering. Esposito and Iervolino (2012), calibrated on the ITACA database, represent a lower-bound estimate of  $\rho(h)$ . A possible explanation can be attributable to the large variability in terms of the magnitudes of the events they considered; indeed, they selected records with Mw ranging from 4.0 to 6.9. Goda and Atkinson (2010) and Heresi and Miranda (2018) feature a different decay with respect to the other models. The main causes probably lie with either the exponential model or the datasets used, making a direct comparison difficult.

## Conclusions

This study focuses on the Mw  $\geq 5.0$  events from the 2016-2017 Central Italy seismic sequence to identify factors that influence the correlation structure of ground motion. We derive a GMPE for each event to be used in the computation of the intra-event residuals and the correlation distance. We use two different estimators to calculate the sample semivariogram and two different approaches to estimate the intra-event standard deviation. An exponential model characterized by two parameters (range and sill) is used to fit each sample semivariogram. The results are rather surprising. Despite considering the same seismic region, the outcomes feature a large variability in terms of correlation distance. The four small events that occurred in January 2017 present larger ranges in comparison to the Mw 6.5 Norcia earthquake. As suggested by Sokolov *et al.* (2012), we interpret these results on account of a high non-random component in the



residuals, which reflects factors, such as path and azimuth effects and spatial variation of soil condition, that are neglected in the GMPE and contribute to a large correlation. Further analyses are required in order to draw firm conclusions and future efforts should be made to investigate: (1) local site effects through the definition of an *ad hoc* site correction for each station; (2) hypothesis of isotropy and stationarity, compared to the concept of anisotropy and non stationarity; and (3) consideration of the nugget effect. In addition, we find a positive correlation between range and the structural period of vibration, as expected from literature. The comparison with other models suggests that a single rate of decay of correlation as a function of the inter-stations distance is not suitable for seismic hazard and risk analysis as the correlation length appears to be regionally-dependent.

These preliminary results could be used to improve seismic loss estimation for spatially distributed infrastructures and portfolios of buildings, as well as for more informed risk management and decision making. The implementation of a logic tree (Sokolov *et al.*, 2012) for correlation models would be suitable in order to account for the high variability in the ranges. We note that at short separation distances (less than 4km) the models are poorly constrained due to a shortage of observations (Goda and Atkinson, 2010; Wagener *et al.*, 2016). Therefore, caution must be applied when adopting these models.

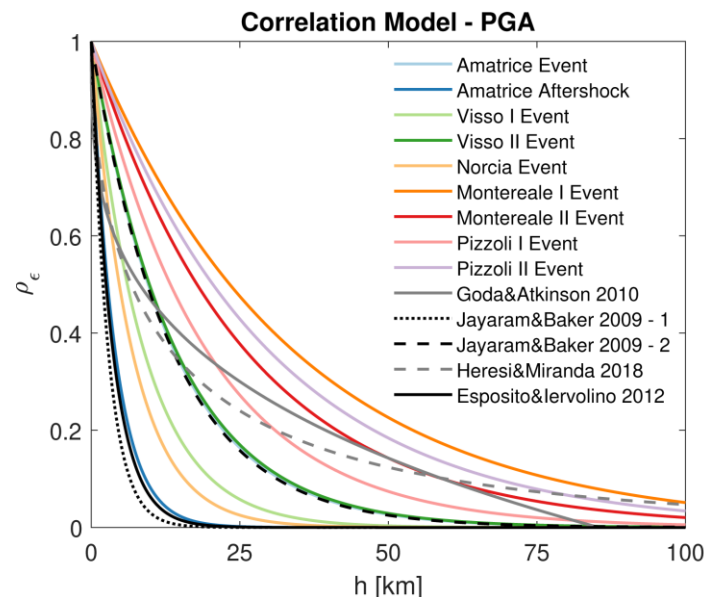


Figure 7: PGA correlation models obtained in this study compared to different correlation models proposed in literature.

## Acknowledgements

We thank Maria D'amico (INGV-Milan) for helping retrieving the dataset related to the events that occurred in January 2017.

## References

- Cheloni, D. et al., 2016. GPS observations of coseismic deformation following the 2016, August 24, Mw 6 Amatrice earthquake (central Italy): data, analysis and preliminary fault model. *Annals of Geophysics*, 59.
- Chiaraluce, L. et al., 2017. The 2016 central Italy seismic sequence: A first look at the mainshocks, aftershocks, and source models. *Seismological Research Letters*, 88, pp. 757.
- Cressie, N., & Hawkins, D. M., 1980. Robust estimation of the variogram. *Journal of the International Association for Mathematical Geology*, 12(2). Cited in Esposito and Iervolino (2011).
- Douglas, J. and Edwards, B., 2016. Recent and future developments in earthquake ground motion estimation. *Earth-Science Reviews*, 160, pp. 203–219. doi: 10.1016/j.earscirev.2016.07.005.
- Esposito, S. and Iervolino, I., 2012. Spatial correlation of spectral acceleration in European data. *Bulletin of the Seismological Society of America*, 102(6), pp. 2781–2788.

- Esposito, S. and Iervolino, I., 2011. PGA and PGV spatial correlation models based on European multievent datasets. *Bulletin of the Seismological Society of America*, 101(5), pp. 2532-2541.
- Goda, K. and Hong, H., 2008. Spatial correlation of peak ground motions and response spectra. *Bulletin of the Seismological Society of America*, 98(1), pp. 354-365.
- Goda, K. and Atkinson, G.M., 2010. Intraevent spatial correlation of ground-motion parameters using SK-net data. *Bulletin of the Seismological Society of America*, 100(6), pp. 3055-3067.
- Goda, K. and Atkinson, G.M., 2009. Probabilistic characterization of spatially correlated response spectra for earthquakes in Japan. *Bulletin of the Seismological Society of America*, 99(5), pp. 3003-3020.
- Heresi, P. and Miranda, E., 2018. Uncertainty in intraevent spatial correlation of elastic pseudo-acceleration spectral ordinates. *Bulletin of Earthquake Engineering*, 17(3), pp. 1099-1115.
- Jayaram, N. and Baker, J.W., 2009. Correlation model for spatially distributed ground-motion intensities. *Earthquake Engineering & Structural Dynamics*, 38(15), pp. 1687-1708.
- Lanzano G, Puglia R, Russo E, Luzi L, Bindi D, Cotton F, D'Amico M, Felicetta C, Pacor F & ORFEUS WG5 (2018). *ESM strong-motion flat-file 2018*. Istituto Nazionale di Geofisica e Vulcanologia (INGV), Helmholtz-Zentrum Potsdam Deutsches GeoForschungsZentrum (GFZ), Observatories & Research Facilities for European Seismology (ORFEUS). PID: 11099/ESM\_flatfile\_2018.
- Luzi, L., Pacor, F., Puglia, R., Lanzano, G., Felicetta, C., D'amico, M., Michelini, A., Faenza, L., Lauciani, V., Iervolino, I., Baltzopoulos, G. and Chioccarelli, E., 2017. The central Italy seismic sequence between August and December 2016: Analysis of strong-motion observations. *Seismological Research Letters*, 88(5), pp. 1219.
- Matheron, G., 1962. *Traité de géostatistique appliquée. 1 (1962)*. Editions Technip. Cited in Esposito and Iervolino (2011).
- Park, J., Bazzurro, P. and Baker, J., 2007. Modeling spatial correlation of ground motion intensity measures for regional seismic hazard and portfolio loss estimation. *Applications of statistics and probability in civil engineering*, pp. 1-8.
- Sokolov, V., & Wenzel, F., 2011. Influence of spatial correlation of strong ground motion on uncertainty in earthquake loss estimation. *Earthquake Engineering & Structural Dynamics*, 40(9), pp. 993.
- Sokolov, V., Wenzel, F., Wen, K.L. and Jean, W.Y., 2012. On the influence of site conditions and earthquake magnitude on ground-motion within-earthquake correlation: analysis of PGA data from TSMIP (Taiwan) network. *Bulletin of Earthquake Engineering*, 10(5), pp. 1401.
- Sokolov, V., Wenzel, F. and Kuo-Liang, W., 2010. Uncertainty and spatial correlation of earthquake ground motion in Taiwan. *TAO: Terrestrial, Atmospheric and Oceanic Sciences*, 21(6), pp. 9.
- Wagener, T., Goda, K., Erdik, M., Daniell, J. and Wenzel, F., 2016. A spatial correlation model of peak ground acceleration and response spectra based on data of the Istanbul earthquake rapid response and early warning system. *Soil Dynamics and Earthquake Engineering*, 85, pp. 166-178.
- Wald, D.J. and Allen, T.I., 2007. Topographic slope as a proxy for seismic site conditions and amplification. *Bulletin of the Seismological Society of America*, 97(5), pp. 1379.
- Wang, M. and Takada, T., 2005. Macrospectral correlation model of seismic ground motions. *Earthquake Spectra*, 21(4), pp. 1137-1156.
- Weatherill, G., Silva, V., Crowley, H. and Bazzurro, P., 2015. Exploring the impact of spatial correlations and uncertainties for portfolio analysis in probabilistic seismic loss estimation. *Bulletin of Earthquake Engineering*, 13(4), pp. 957-981.
- Weatherill, G., Esposito, S., Iervolino, I., Franchin, P. and Cavalieri, F., 2014. Framework for seismic hazard analysis of spatially distributed systems. *SYNER-G: Systemic Seismic Vulnerability and Risk Assessment of Complex Urban, Utility, Lifeline Systems and Critical Facilities*. Springer, pp. 57-88.
- Webster, R., & Oliver, M. A., 2007. *Geostatistics for environmental scientists*. John Wiley & Sons.
- Zerva, A. and Zervas, V., 2002. Spatial variation of seismic ground motions: an overview. *Applied Mechanics Reviews*, 55(3), pp. 271.